

The Oculomotor Neural Integrator Uses a Behavior-Related Coordinate System

J. Douglas Crawford

Department of Neurophysiology, Montreal Neurological Institute, McGill University, Montreal, Quebec, Canada H3A 2B4

Coordinate systems are a central issue in computational neuroscience: are they explicitly represented at some reductive level of brain function, and if so, are they only trivial products of associated anatomic geometries? This investigation examined these questions in the neural network that holds eye position, the so-called *oculomotor integrator*. Since neural activity in the integrator is behaviorally constrained by *Listing's law* to encode horizontal and vertical eye positions within *Listing's plane* and zero rotation about the orthogonal *torsional* axis, it was hypothesized that any integrator coordinate system would be developmentally predisposed to align with Listing's plane. A test for this hypothesis was developed with the use of a kinematically correct model of the three-dimensional saccade generator. Three mathematical integrators were used to represent the neuron populations that control torsional, vertical, and horizontal eye position. Simulated failure of the torsional and vertical integrators produced eye position drift that was parallel to the horizontal plane containing the intrinsic coordinate axes for these components. Furthermore, this drift settled toward a resting range parallel to the intrinsic vertical coordinate axis (for horizontal rotation).

To experimentally identify these intrinsic population coordinates, three-dimensional eye positions were measured in four *Macaca fascicularis* after injection of muscimol into the mesencephalic interstitial nucleus of Cajal (INC), a technique that disrupts the torsional and vertical integrators (Crawford et al., 1991). INC inactivation produced exponential, position-dependent decay in vertical and torsional eye position. There was no position-dependent horizontal drift, but in the original coordinate system (defined arbitrarily by the measurement apparatus) there was a constant-direction horizontal drift. However, this extraneous horizontal drift was eliminated when the data were transformed into a coordinate system that aligned with Listing's plane. The direction of torsional drift correlated well ($r = 0.85$), across all experiments, with the normal to Listing's plane. On average, these two directions were only 0.06° from perfect alignment. In

contrast, drift direction did not correlate with stereotaxic coordinates ($r = 0.10$). Furthermore, the drift settled toward a range parallel to and correlated with Listing's plane ($r = 0.94$), whereas this range did not correlate well with stereotaxic coordinates ($r = 0.02$). On average, the resting range was aligned within 0.98° of Listing's plane. Finally, this resting range was near orthogonal (average 91.9° across all experiments) to the direction of torsional drift.

These results show that integrator cell populations use an orthogonal, craniotopic coordinate system that aligns with Listing's plane. This suggests that intrinsic brain coordinates are not just a trivial product of anatomy, but instead are optimally suited for the generation of specific behaviors. Measurement and simulation of motor impairment in arbitrary coordinate systems is expected to yield misleading results, but the present investigation suggests that the configurations and orientations of some intrinsic coordinate systems may be inferred from noninvasive behavioral measurements.

[Key words: oculomotor, integrator, coordinate system, kinematics, three-dimensional, interstitial nucleus of Cajal, monkey]

Coordinate systems are indispensable to the study of motor control because they are implicit in our basic intuitions of horizontal and vertical movement. For example, what is a horizontal eye movement? Horizontal eye movement can be defined as rotation of the eye about a specific vertical *coordinate* axis, but this axis could be embedded in the eye, space, or the head. Even when the latter *reference frame* is specified, the coordinate for horizontal rotations could still be chosen from an infinite set of roughly "vertical" orientations, for example, orthogonal to the stereotaxic horizontal plane, or tilted farther back like the axis of rotation controlled by the horizontal eye muscles. What is pure horizontal rotation in any one of these coordinate systems will be partially horizontal and partially *torsional* rotation in the other coordinate systems (Fig. 1). Thus, a bewildering menu of coordinate systems is available to (1) experimenters and clinicians, who must measure and describe the direction of movements, and (2) theoretical investigators who model neural control systems with the use of mathematical operators that require explicit coordinate systems.

Clearly investigators of motor control will often want to use coordinate systems that are physiologically meaningful, in the sense that they align with those used by the brain. However, the use of coordinate systems by the brain itself has been an issue of contention between two schools of thought. The first view, which has often dominated theoretical discussions of brain function over the last decade, posits that explicit coordinate systems and coordinate transformations are an important, in-

Received Dec. 15, 1993; revised May 3, 1994; accepted May 11, 1994.

I thank Drs. T. Vilis and D. Tweed for their valuable critical comments. T. Vilis, L. Van Cleef, S. Watts, S. Nicol, and G. Santor of the Department of Physiology, University of Western Ontario were instrumental for the experimental component of this study, which was supported by Medical Research Council of Canada Grant MT9335. The theoretical and analytical portions of this study were supported by a Medical Research Council of Canada Fellowship.

Correspondence should be addressed to J. Douglas Crawford, Department of Neurophysiology, Montreal Neurological Institute, McGill University, 3801 University Street, Montreal, Quebec, Canada H3A 2B4.

Copyright © 1994 Society for Neuroscience 0270-6474/94/146911-13\$05.00/0

tegral aspect of brain function (e.g., Robinson, 1985; Simpson and Graf, 1985; Soechting and Flanders, 1992; Masino and Knudsen, 1993). The second view, championed by neural network modelers, questions the existence of such intrinsic brain coordinate systems (Robinson, 1992). This is because connectionist neural networks can control movements without using discrete coordinate systems; that is, directional commands are so variable and distributed within these networks that there are no distinct groupings of movement commands along cardinal directions. Since real neurons show similar variations, it has been suggested that the brain cannot be understood in terms of "black box" operations in explicit coordinate systems (Robinson, 1992).

These two views of neural coordinate systems can be exemplified in the neural network that holds eye position during visual fixation. This network is called the *neural integrator* because it is thought to derive the eye position command from eye movement commands using a process equivalent to mathematical integration (Robinson, 1968, 1975, 1987). Several experiments in monkeys and cats suggest that the nucleus prepositus hypoglossi region is the integrator for horizontal eye position; in particular, pharmacological inactivation of neurons in this region produced a failure to hold eccentric horizontal eye positions, manifested as a centripetal drift, with little or no vertical drift (Cannon and Robinson, 1987; Cheron and Godaux, 1987; Straube et al., 1991; Yakota et al., 1992). The mesencephalic interstitial nucleus of Cajal (INC), which flanks the anterior pole of the third cranial nucleus bilaterally, appears to be a critical site for the integration of vertical and torsional eye position. In particular, pharmacological inactivation of the monkey INC caused a failure to hold vertical and torsional eye positions with little or no horizontal drift (Crawford et al., 1991; Crawford and Vilis, 1993).

Further experiments have revealed the intrinsic organization of torsional and vertical eye position signals within the INC. Single-unit recordings suggest that there are two intermingled populations of neurons on each side of the INC, one with activity that correlates with upward eye position and one that correlates with downward eye position (King et al., 1981; Fukushima et al., 1990b). However, the vertically tuned neurons on the right side of the INC also correlate to clockwise (CW) rotations of the eye, and the neurons on the left side also correlate to counterclockwise (CCW) rotations (Fukushima et al., 1990a). Unilateral stimulation of the right and left sides produces primarily CW and CCW rotations, respectively, whereas unilateral damage causes torsional eye position to shift in the opposite direction (Crawford et al., 1991; Crawford and Vilis, 1993). Thus, the INC can be divided into four populations of neurons, two for control of CW-up and CW-down position components on the right side of the brain, and two for control of CCW-up and CCW-down components in the left INC. This resembles the anatomic coordinates of the extraocular muscles and semicircular canals, which combine control of torsional and vertical eye rotations in a similar manner, and control horizontal rotations independently (Ezure and Graf, 1984).

Such observations have fostered a debate whether premotor oculomotor structures use coordinates that align best with those of the canals, a prominent source of input (Robinson and Zee, 1981) or with those of the eye muscles that they control (Büttner et al., 1977). Unfortunately, single-unit recordings showed that activity of neurons in the nucleus prepositus hypoglossi area and INC sometimes correlated best with the muscle directions,

sometimes with canal directions, and generally showed random variations (Baker et al., 1975; King et al., 1981; Fukushima et al., 1990a). However, *if* this network is divided into functionally independent integrators for horizontal and vertical/torsional, then we can define its coordinate system by the overall output of the populations within each of these separate integrators and ignore variations between individual neurons within the population. This level of analysis is clearly of more relevance to practical questions such as "does damage to the INC cause horizontal eye position drift?" The answer to this question will depend on one's definition of horizontal eye position with respect to the eye position coordinates determined by the overall outputs of entire INC cell populations. However, there would be little practical or theoretical advantage in determining such a population coordinate system unless it was consistent between subjects with respect to some measurable, physiologically meaningful variable. Furthermore, since this variable has generally been assumed to be either the muscles or canals, some investigators have dismissed oculomotor coordinate systems as a trivial by-product of anatomic geometries (Robinson, 1992; Soechting and Flanders, 1992).

From a computational standpoint, the integrator could utilize any coordinate system, or none at all, as long as it makes the correct synaptic connections to the downstream motoneurons. However, from a developmental standpoint, one would predict that neural activity within the integrator itself would contribute to the development and ongoing maintenance of the synaptic connections that underlay integrator coordinates (Shatz, 1992). Such developmental considerations may in part explain the resemblance of integrator coordinates to those of the semicircular canals, which constitute a major input to this structure. However, there is another, more stringent constraint on integrator activity. Saccades (rapid eye movements with the head still) and slow tracking movements called smooth pursuit are constrained by Listing's law (von Helmholtz, 1867; Ferman et al., 1987; Tweed and Vilis, 1990a; Straumann et al., 1991; Minkin et al., 1993). Listing's law states that the eye may only assume positions that can be reached from a given reference eye position by a rotation about an axis that lies in a head-fixed plane. For one particular reference position, called primary position, the direction of gaze is orthogonal to the associated plane, which is called Listing's plane. If eye position is represented in a coordinate system in which the torsional axis is parallel to the primary gaze direction, Listing's law simply states that eye position is constrained to zero torsion (Westheimer, 1957). Several observations show that Listing's law is not a trivial muscular constraint, but rather a behavioral strategy. For example, (1) the orientation of Listing's plane varies with respect to anatomic landmarks (Tweed and Vilis, 1990a; Crawford and Vilis 1992), even within one subject over time (von Helmholtz 1867; Ferman et al., 1987), and (2) Listing's law is not obeyed by slow phases of the vestibulo-ocular reflex, although large accumulations of torsion are prevented by the intervening fast phases (Crawford and Vilis, 1991). Since the neural integrator is normally constrained to encode zero torsion in Listing's coordinates, and since such neural activity has been observed to affect synaptic organization in other systems (Shatz, 1992), it is reasonable to hypothesize that this constraint will influence the synaptic connections that determine integrator coordinates.

The present investigation utilized pharmacological inactivation of the INC and precise measurement of eye rotation axes to investigate the overall coordinate axes controlled by sub-

populations of cells in the oculomotor integrator. Pharmacological inactivation was used because, unlike single-unit recording and electrical stimulation, respectively, this technique gives a causal indication of the overall output of a large number of local cell bodies (electrical stimulation is insufficient because it may orthodromically activate fibers of passage and antidromically activate inputs to the INC that affect eye movements through other pathways). The potential of this technique has remained untapped because previous investigations made no attempt to precisely define the directions of horizontal, vertical, or torsional drift observed during integrator failure (Cannon and Robinson, 1987; Cheron and Godaux, 1987; Crawford et al., 1991; Straube et al., 1991; Yakota et al., 1992; Crawford and Vilis, 1993). This investigation rigorously tested the coordinates of eye position deficits observed during INC inactivation against the predictions of a kinematically correct model of the three-dimensional saccade generator. The results suggest that a consistent coordinate system does exist at the level of integrator cell populations, and this coordinate system is not just a trivial by-product of anatomic geometries. Rather, it appears that the integrator uses the coordinate system that best suits the behavior that it generates.

Materials and Methods

Measurement of three-dimensional eye positions. Three-dimensional eye movements were recorded from four *Macaca fascicularis*, coded BAR, LAR, CAS, and ART, using the dual search coil/quaternion technique (Tweed et al., 1990). Each monkey underwent surgery under aseptic conditions and pentobarbital anesthesia in preparation for chronic behavioral experiments. During surgery a skull cap composed of dental acrylic was fastened to the animal's head, and two enamelled copper search coils of 5 mm diameter were implanted in one eye for measurement of three-dimensional eye position. In two of the animals (CAS and ART), coils were implanted in both eyes. Wire leads from the coils were extended temporally beneath the conjunctiva and then subcutaneously to sockets secured on the cap. During experiments, the head of the alert monkey was immobilized by fixing the skull cap near the center of three orthogonal magnetic fields. These fields were in phase, but operated at different frequencies (62.5, 125, and 250 kHz). These fields induced electrical currents in the eye coils, proportionate to their orientation, that were digitized by a computer at a sampling frequency of 100 Hz. During experiments these signals were recorded in 100 sec files, while the animal made saccades between hand-held visual targets placed to reveal the full range of obtainable eye positions.

In order to examine the central hypothesis of this article a simple and accurate representation of three-dimensional eye position was required. Therefore, the computer was used to convert coil signals into eye position quaternions, both on-line and off, using a method described previously (Tweed et al., 1990). Quaternions are composed of a scalar part q_0 , and a vector part \mathbf{q} . It is the vector part that is used for representation of data. The direction of vector \mathbf{q} gives the axis of the rotation that would take the eye from a reference position to the current position, and the length of \mathbf{q} is a function of the magnitude of this rotation. To be precise, the quaternion vector is related to the axis and magnitude of such a rotation as follows:

$$\mathbf{q} = \mathbf{n} \sin(\alpha/2) \quad (1)$$

The angle α is the magnitude of the rotation and \mathbf{n} is a three-dimensional unit vector parallel to the axis of rotation (Tweed and Vilis, 1987). Thus, \mathbf{q} is composed of three components which give the torsional, vertical and horizontal displacement of the eye from reference position. At reference position $\alpha = \text{zero}$ and thus $\mathbf{q} = \text{zero}$. Angular eye velocities are easily computed from these position quaternions by dividing a given quaternion by the previous quaternion, and then differentiating the resultant displacement quaternion with respect to time (Crawford and Vilis, 1991). Detailed discussions of eye position quaternion recording and mathematics are available elsewhere (Westheimer, 1957; Tweed and Vilis, 1987; Tweed et al., 1990; Crawford and Vilis, 1991).

Coordinate systems for data representation. This investigation required that eye position quaternions be analyzed and plotted in three

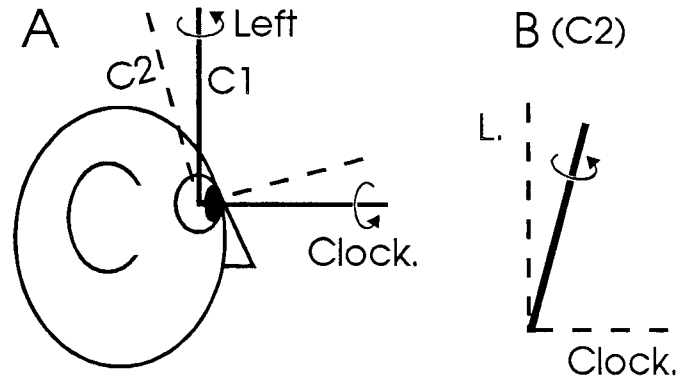


Figure 1. A, Description of eye rotations in two separate orthogonal head-fixed coordinate systems. In coordinate system 1 ($C1$, solid lines), the vertical coordinate axis is arbitrarily set parallel to the earth vertical axis when the head is in a normal upright orientation. In coordinate system $C1$, pure horizontal rotation signifies rotation about this vertical axis. *Torsion* is defined as rotation of the eye about the orthogonal, forward-pointing axis, where clockwise and counterclockwise rotation are defined from the subject's point of view. The second head-fixed coordinate system ($C2$, dashed line) is rotated 15° upward from $C1$. B, When a purely leftward rotation about the vertical coordinate axis in $C1$ (solid line) is plotted in coordinate system $C2$, it now has both leftward and clockwise components.

coordinate systems based on (1) the magnetic fields, (2) the stereotaxic planes, and (3) Listing's plane. In all cases the head was the frame of reference, for example, torsion is defined to be rotation about an axis fixed with respect to the head, as in Figure 1, rather than rotation about the line of sight. At the beginning of each experiment the range of eye coil signals were recorded during head-fixed saccades as a control. In addition, eye position was recorded while the animal looked along the direction of the forward-pointing magnetic field for use as provisory reference position. Quaternions computed directly from this data were, by default, in coordinates defined by the magnetic fields, that is, the torsional, vertical, and horizontal axes were parallel with the field directions. This *field coordinate system* was arbitrary, since it relied on placement of the animals at our best estimate of an upright position.

As required by Listing's law, the range of eye positions relative to the provisory reference position conformed to a plane. This *displacement plane* was not Listing's plane, unless the reference position coincided with primary position (von Helmholtz, 1867; Tweed and Vilis, 1990a), and tended to tilt from the plane of the vertical and horizontal field coordinates. However, the laws of rotational kinematics require that Listing's plane will tilt in the same direction as this plane, but by twice as much (Tweed and Vilis, 1990a). This law was used to determine the orientation of Listing's plane and thus primary position by a method described previously (Tweed et al., 1990). As defined originally, primary position is the unique reference position where gaze is orthogonal to the associated displacement plane, which is Listing's plane (von Helmholtz, 1925; Tweed and Vilis, 1990b). Once primary position had been computed, it was consistently used as the reference position. This ensured that the control range of data was always a true Listing's plane, and that data did not vary as a kinematic artifact of using different reference positions in different coordinate systems.

After computing the primary position, eye positions relative to this position were plotted either in the original arbitrary field coordinates, or in Listing's coordinates. By this one means a system with vertical and horizontal coordinates aligned in Listing's plane, and the torsional coordinate parallel with the primary gaze direction. In a third coordinate system, data were rotated so that the vertical and horizontal coordinate axes aligned with the coronal stereotaxic plane. The orientation of the stereotaxic planes was recorded during experiments in the first two animals (BAR and LAR) by measuring the angle between a line from the center of the external auditory canal to the orbital canthus, and the horizontal field direction. In the other animals search coils that were aligned with the stereotaxic horizontal and sagittal planes were implanted in the skull cap.

Invasive neurophysiological procedures. Before initiating experiments, a stainless steel recording chamber was mounted stereotaxically over a

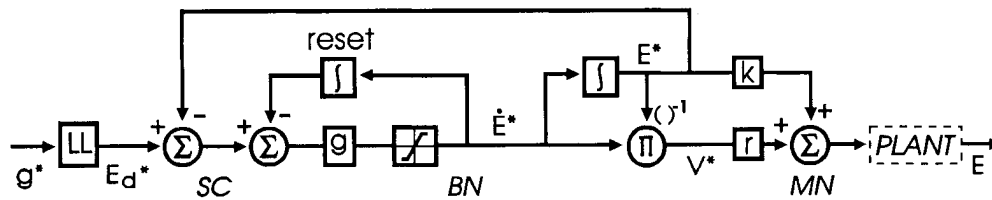


Figure 2. A theoretical model for the generation of kinematically correct saccades in three dimensions. *Asterisks* denote internal kinematic representations. *From left*, desired gaze direction (g^*) is input into the Listing's law operator (LL) (Tweed and Vilis, 1990b), which computes the corresponding unique desired eye position (E_d^*) on Listing's plane (this is the point where the fundamental constraint imposed by Listing's law is implemented). A representation of current eye position (E^*) is subtracted from E_d^* to compute the initial desired change in eye position. The superior colliculus (SC) only encodes position change vectors parallel to Listing's plane (Van Opstal et al., 1991); that is, any torsional components must be encoded in a separate channel in parallel with the superior colliculus. This vector signal is amplified by a gain factor (g), and goes through a normalizing saturation to produce the drive to burst neurons (BN). These burst neurons encode the first derivative of eye position with respect to time (\dot{E}^*), which is a command encoding rate of eye position change. Saccades are guided and terminated by a "local" feedback loop that is composed of a resettable (*reset*) integrator (J) that receives the BN output, converts it to displacement, and then subtracts this from the initial desired position change until the target is reached (Jürgens et al., 1981). In the "indirect pathway" E^* is integrated (J) to produce the neural command for current eye position (E^*). *The coordinate system used in the latter integration step is the focus of the present investigation.* E^* is then multiplied by a gain element (k) to match it to the plant's elasticity, and finally input to the motoneurons (MN). In the "direct pathway" of burst neuron inputs to motoneurons, \dot{E}^* is divided by E^* to produce the eye angular velocity signal V^* . This is the point where the position-dependent saccade axis tilts required by Listing's law (Tweed and Vilis 1990a) are implemented (for a review of the multiplicative relationship between V and E in rotations, see Tweed and Vilis, 1987). V^* is amplified by a gain factor (r) to match the viscosity of the plant, and then input to the motoneurons. The motoneuron output enters the plant (the eye and its muscles) to produce eye position (E), as described in Crawford and Vilis (1991).

trephine hole in the skull centered at 8 mm anterior and 0 mm lateral, directly over the INC (Shantha et al., 1968). During experiments a hydraulic microdrive attached to the recording chamber was used to advance monopolar tungsten electrodes (Frederick Haer; 4 M Ω) which were used to record from units and to stimulate. The electrode was inserted in an insulated guide cannula, which was manually advanced into the brain stem to within 5 mm of the selected oculomotor region. Subsequently the electrode was hydraulically advanced by as much as 10 mm from the guide cannula. Units were identified by comparing their discharge patterns with eye movements and positions. Afterward the same electrode was used to microstimulate the region at 0.5 mm vertical intervals using monophasic cathodal square pulses delivered at 20 μ A and 200 Hz for durations of 300–600 msec.

After recording and stimulating, the electrode was pulled out of its guide tube without otherwise disturbing the tube or the microdrive, and a 30 gauge cannula (Small Parts Inc.) was then inserted into the guide tube and lowered to a depth determined during the unit recording and stimulation phases, usually just above the selected oculomotor region. A Hamilton syringe which was used to deliver 0.3 μ l of a 0.05% muscimol solution (Sigma). Muscimol has a powerful inhibitory effect on neurons which possess γ -aminobutyric acid (GABA) receptors. Thus, muscimol should inhibit action potential generation in local cell bodies without disrupting fibers of passage. Eye movement recordings commenced immediately after the injection and continued for 30 min or more. Afterward, the animal was allowed a 48 hr recovery period (slight residual effects were sometimes observed after 24 hr) and then experiments were repeated at an adjacent brain site displaced lateral-medial or rostral-caudal by 1 mm.

In the above fashion the INC and surrounding regions were thoroughly explored over the course of several months in each animal. Experiments were terminated if the animal's control data showed signs of eye movement deficits, presumably from long-term effects of repeated electrode penetrations. The criteria used to establish injection controls and to identify the INC have been published elsewhere (Crawford et al., 1991; Crawford and Vilis, 1992, 1993) In brief, the INC was functionally identified as the unique midbrain region where unit activity correlated to vertical eye position (King et al., 1981; Fukushima et al., 1990b), unilateral stimulation produced ipsi-torsional eye movements that held their final position (Crawford et al., 1991), and muscimol injection produced a failure to hold vertical and torsional eye positions (Crawford et al., 1991; Crawford and Vilis, 1993).

When the midbrain oculomotor region had been thoroughly explored, the animals were deeply anesthetized with pentobarbital and electrolytic lesions (1.5 mA DC anodal current for 15 sec) were made at a reference microdrive coordinate. Immediately afterward animals were given a lethal dose of anesthetic and perfused with an intra-aortic injection of formalin. The brains were removed, sliced into 100 μ m sections, and

stained with thionine. The resulting slides were compared to a stereotaxic atlas of the monkey brain (Shantha et al., 1968) to histologically confirm our functional identification of the INC.

Simulation of integrator failure in arbitrary intrinsic coordinate systems. In order to establish a solid theoretical basis for analysis of the data, three-dimensional neural integrator failure was simulated on a computer. Specifically, the purpose of the theoretical component of this study was to develop a direct test for the intrinsic coordinates of the integrator that could be applied to eye position data collected during INC inactivation. To put the simulated integrator deficit into the correct behavioral context, the integrator was placed within a kinematically correct model that generates saccades toward eye positions in Listing's plane (Fig. 2). The model was designed to use mechanisms consistent with the known neurophysiology of the three-dimensional saccade generator (Van Opstal et al., 1991), and was implemented with the use of quaternions (simply because of their convenience in representation of three-dimensional eye positions and in handling the mathematical properties of three-dimensional rotations). However, with the exception of the velocity-to-position integrator, the internal workings of this model are inconsequential to the present investigation.

Initially, all of the mathematical operations in the model were performed in a coordinate system aligned with Listing's plane. This made the model simpler, because coordinate transformations between mathematical modules became a trivial mapping of torsion-to-torsion, vertical-to-vertical, and horizontal-to-horizontal components. Use of Listing's coordinates, even in the plant, is valid because it is both arbitrary and transparent as long as all internal modules function correctly.

Integration in itself is a one-dimensional computation. Therefore, three integrators were needed for the torsional, vertical, and horizontal dimensions of eye movement. Each integrator was simulated using

$$q_{\text{new}} = (q_{\text{old}} + \Delta t \times \dot{q} + \beta) \times (1 - \text{leak}), \quad (2)$$

where q is one component of a position quaternion (the output), \dot{q} is the rate-of-position-change command (the input) along the corresponding dimension, Δt is the time interval represented by each iteration of the program, and β and *leak* are constants equal to zero in the normal case. Integrator failure (due to INC inactivation) was simulated by setting the leak constant of the torsional and vertical integrators at a value between 0 and 1.

Previous experiments have shown that during integrator failure the eye does not always drift toward a consistent "zero" value, but rather drifts toward a resting value or range that may be shifted to varying degrees depending on the nature of the neural damage (Cannon and Robinson, 1987). For example, unilateral inactivation of the INC produced shifts in the torsional resting position (Crawford and Vilis, 1993). These torsional shifts were simulated in the present investigation by introducing a non-zero β value in the torsional integrator.

In order to evaluate the relationship (if any) between the intrinsic coordinates of the integrator and the drift produced by integrator failure, the latter was simulated in arbitrary intrinsic coordinate systems. This was implemented by multiplying the integrator's input vector (T, V, H) by a matrix whose columns were unit vectors parallel to Listing's coordinates but expressed in the coordinate system of the integrator. For example, the following matrix multiplication was used for an orthogonal integrator coordinate system (INT) that is rotated θ upward about the horizontal axis from Listing's coordinates (LIST):

$$\begin{matrix} T_{(INT)} \\ V_{(INT)} \\ H_{(INT)} \end{matrix} = \begin{matrix} \text{Cosine } \theta & 0 & \text{Sine } \theta \\ 0 & 1 & 0 \\ -\text{Sine } \theta & 0 & \text{Cosine } \theta \end{matrix} \times \begin{matrix} T_{(LIST)} \\ V_{(LIST)} \\ H_{(LIST)} \end{matrix} \quad (3)$$

The outputs of the integrator were then multiplied by the inverse of the above matrix to "undo" the first coordinate transformation. To rotate only the torsional axis upward, the third column of the matrix in Equation 4 was changed to (0,0,1), and its inverse recomputed. Similarly, to rotate only the vertical axis backward, the first column of the matrix was changed to (1,0,0) and its inverse recomputed. Similar matrix operations can be used to rotate the integrator coordinates 45° horizontally to achieve a more realistic combination of torsional and vertical integrators. However, this transformation had no effect on simulations in which the torsional and vertical integrators are made to leak equally.

Clearly, similar simulations of integrator failure may be performed using any two-dimensional or three-dimensional model that uses integrators to generate the eye position signal. The above methods for simulating integrator failure depended on only two assumptions: (1) the integrators for torsional and vertical eye position could be inactivated without affecting the horizontal integrator, and (2) these three integrators each encode eye position about a head-fixed axis. These assumptions were examined experimentally (see Results) before the theoretical coordinate dependencies of integrator failure were compared to the experimental data.

Results

Coordinate dependencies in the eye position drift

As reported previously, injection of muscimol into the INC caused vertical and torsional eye positions to decay at an exponential rate. This is illustrated in Figure 3A, which plots the torsional (T), horizontal (H), and vertical (V) components of eye position vectors as a function of time, 38 min after unilateral injection of muscimol into the INC. Positions were computed relative to primary position in a coordinate system aligned with the magnetic field directions of the measurement apparatus. Torsional eye position drifted exponentially (thicker line segments), clockwise in this example, whereas the intervening resetting rapid eye movements (thinner segments) had the opposite torsional component. There was also a postsaccadic vertical drift, and most surprisingly, a small but consistent postsaccadic horizontal drift.

By eliminating the time variable, component versus component plots can be made of eye position vectors that more clearly show the direction of drift in a much larger amount of data. Figure 3B shows data from the same experiment as Figure 3A, now plotting horizontal position versus vertical position. Each line is composed of eye positions that are really the tips of position vectors, plotted so that up on the figure corresponds to upward gaze etc. Rapid eye movements have been eliminated from this figure so that only sequences of eye positions during postsaccadic drift are illustrated, and open circles at the final positions of each sequence indicate the direction of drift. In this plot two things are clear: there was a position-dependent drift of vertical position toward center, and there was a consistent leftward postsaccadic drift. Horizontal eye position decayed exponentially and settled very rapidly (Fig. 3A). However, it did not show the horizontal position dependence expected from

horizontal integrator failure, that is, the rate of horizontal drift did not depend on initial horizontal eye position (Fig. 3B), and it settled toward a different horizontal resting point after each saccade (Fig. 3A).

Figure 3C plots the same data as Figure 3A, but now in a coordinate system where the vertical and horizontal axes are aligned in Listing's plane. Note that in this coordinate system the slope of the torsional drift increased slightly, but the horizontal drift disappeared. When the data from Figure 3B was transformed into Listing's coordinates (Fig. 3D), the horizontal drift was largely eliminated throughout the position range. Figure 3 serves to exemplify the type of cross-talk that can occur between directions of drift when presented in an arbitrary coordinate system. In some experiments (where the magnitude of torsional drift was much greater than that of vertical drift), the horizontal drift was more prominent than the vertical drift (when plotted in arbitrary field coordinates). However, it will become clear below that this surprisingly large horizontal drift was an artifact of plotting eye position in the wrong coordinate system. Basic geometry (Fig. 1) requires that such extraneous horizontal drift (e.g., in Fig. 3A,B) will increase with the magnitude of torsional drift multiplied by the sine of the angle by which the arbitrary data coordinate system is rotated from the intrinsic coordinate system of the integrator. Figure 3 suggests that this latter coordinate system might align with Listing's plane, but more direct tests were required to confirm this hypothesis.

Developing a test for intrinsic integrator coordinates

This theoretical section describes the results of simulating neural integrator failure in various intrinsic coordinate systems. These theoretical results will then be used as a basis to experimentally test intrinsic integrator coordinates. Specifically, these tests formalized the following intuition: if the vertical and torsional integrators have failed, then eye position vectors should fail to hold parallel to the plane that contains the intrinsic integrator coordinates for these position components, but *will hold parallel to the axis that is the intrinsic coordinate axis for horizontal eye position*.

Figure 4 illustrates several horizontal versus torsional plots of simulated normal eye positions (the tips of position vectors emanating from the origin) in Listing's plane. These eye position vectors are plotted relative to primary position in a coordinate system aligned with Listing's plane. In contrast to the previous figure where position plots corresponded to gaze direction, this figure plots horizontal position along the vertical axis of rotation. In addition to being more technically correct (because eye position vectors are parallel to the axis of rotation), this convention simplifies examination of coordinates axes. This is because the data coordinate axes are now plotted in their actual orientation, for example, the vertical axis for horizontal rotation is vertical with respect to the head caricature (Fig. 4). In the illustrated case, the torsional axis points forward, as if one were viewing Listing's plane from the subject's right side. The right-handed convention is used for plotting data, so that pointing the thumb of the right hand from the origin toward a given data point causes the fingers to curl in the direction that the eye is displaced from primary position. In all simulations (Fig. 4A–E) saccades (not shown) were made toward a series of eye positions spaced at 3° horizontal intervals in Listing's plane (only positions during fixation periods are shown). In Figure 4A the integrator was completely intact and positions between saccades held steady in Listing's plane. An identical simulation could be generated

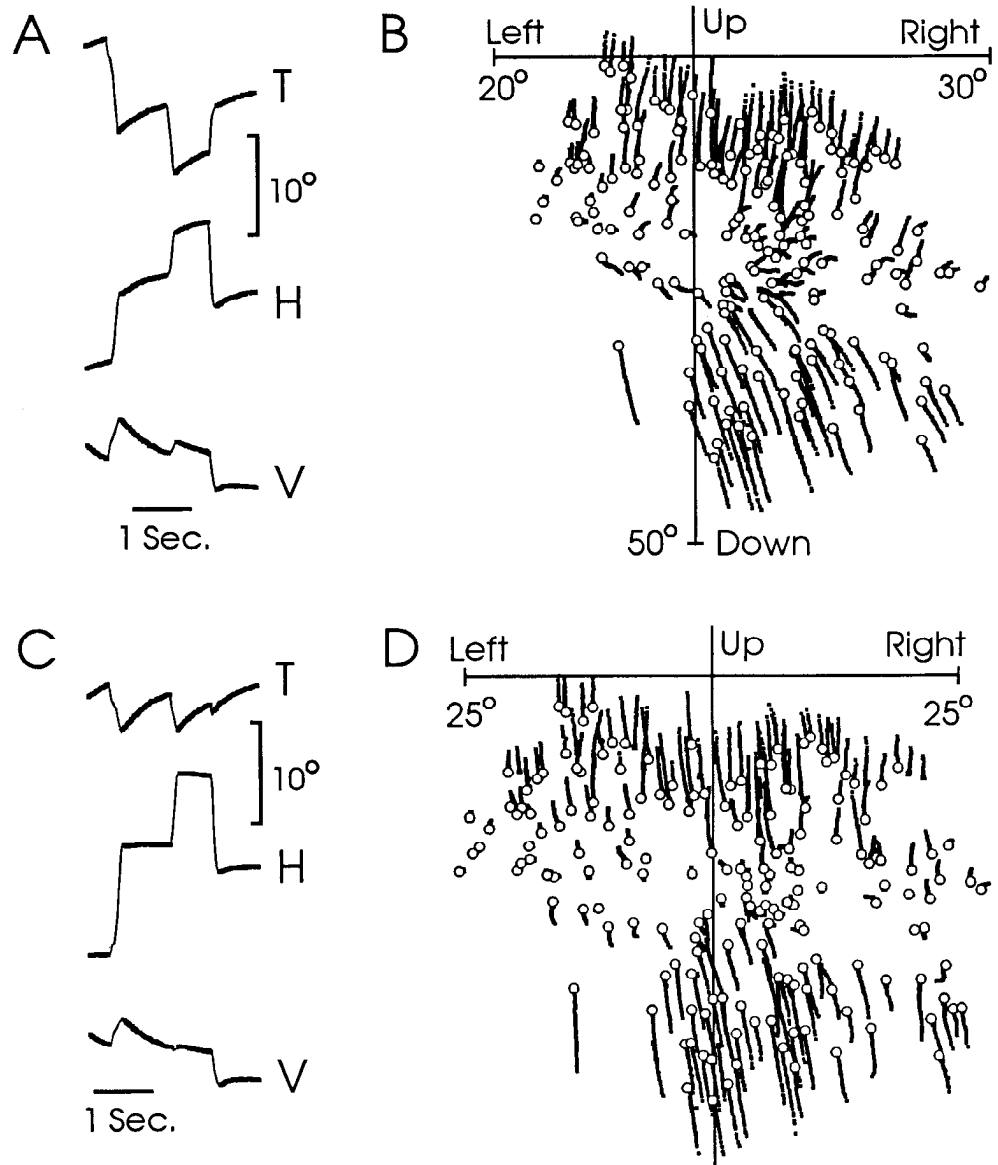


Figure 3. Ocular drift 38 min after a single injection of muscimol into the INC. *A*, Torsional (*T*), horizontal (*H*), and vertical (*V*) eye positions (relative to primary position) are plotted as a function of time. Upward movement on the page denotes clockwise, upward, and leftward movement, respectively. The coordinate axes for these positions aligned with the magnetic field directions. *B*, Horizontal positions plotted as a function of vertical positions recorded over a 100 sec interval. Positions during saccades have been omitted, and *open circles* have been placed at the end-point of each drift sequence. Data are again plotted in magnetic field coordinates. *C* and *D*, The same data after rotation into Listing's coordinates.

using any intrinsic integrator coordinate system, as long as the correct coordinate transformations were made. Thus, integrator coordinates were “invisible” during normal, ideal behavior.

Integrator coordinates were no longer invisible when the integrator malfunctioned. Figure 4*B* shows the effect of damaging the torsional (and vertical) integrators with an intrinsic coordinate system that aligned with Listing's plane. Since the vertical drift is not visible from the perspective used in Figure 4, only the direction of torsional and horizontal drift will be discussed. A torsional offset was introduced in the integrator so that the simulated eye drifted clockwise toward a torsionally shifted range (vertical dashed line) of stable positions. This closely resembles the drift previously reported immediately after injection of muscimol into the INC and is thought to be the underlying mechanism of this drift (Crawford et al., 1991; Crawford and Vilis, 1993). Between these sequences of drift, counterclockwise directed saccades (not shown) brought the eye back toward Listing's plane, resulting in a torsional nystagmus. Note two important observations: first, the direction of drift in Figure 4*B* was orthogonal to Listing's plane, and second, the line of stable

resting points (vertical dashed line) was parallel to Listing's plane. To illustrate that these were not trivial events, Figure 4*C* shows the same simulation, but with an intrinsic coordinate system (thick lines) rotated 15° upward about the origin. In this case, the line of stable positions (dashed line) and the direction of torsional drift both rotated upward by exactly 15°. In Listing's coordinates, as illustrated, it would appear that the eye drifted leftward, in addition to drifting torsionally and vertically. Thus two sets of data, direction of drift and the line of stable positions, should show a nontrivial alignment with the intrinsic coordinates of a malfunctioning neural integrator.

This was further refined into two separate tests of integrator coordinates. In the first two drift simulations (Figs. 4*B,C*) direction of drift and the line of stability were mutually orthogonal. This orthogonality occurred specifically because the coordinate system of the integrator was intrinsically orthogonal in both cases. In Figure 4*D* only the intrinsic vertical coordinate (thick line) was rotated out of Listing's coordinates, producing a non-orthogonal coordinate system. In this case, the line of stable positions (dashed line) rotated by about the same amount,

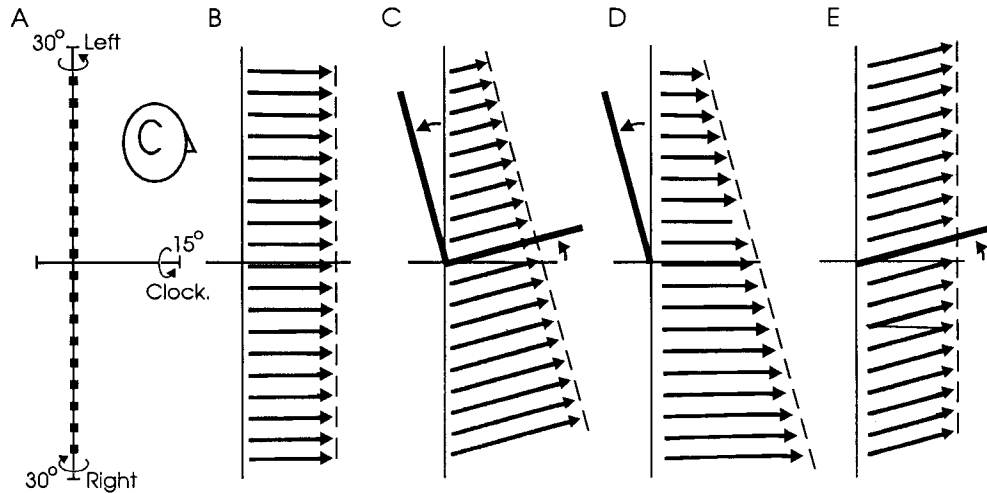


Figure 4. Computer simulations of integrator failure using various intrinsic coordinate systems. Simulated eye position vectors are viewed as if from the subjects right side (see head caricature), so that horizontal position (along the vertical axis) and torsional position are visible. Simulated data are plotted in a coordinate system aligned with Listing's plane. *A*, Normal eye positions in Listing's plane. The model was made to generate a series of 3° horizontal saccades starting from a rightward position. Only positions between movements are shown. *B*, Same simulation, but now the torsional and vertical integrators have been made to leak with a 100 msec time constant, and the integrator is given a torsional bias. This bias determined the torsional offset in the final resting points of the drift (vertical dashed line). The magnitude or direction of this offset was irrelevant for our integrator coordinate test as long as it was sufficiently shifted from the saccade end-points to reveal the direction of drift. This drift direction is indicated by arrowheads placed at the final position of each drift sequence. *C*, Same as previous simulation, but now the intrinsic integrator coordinates (thick lines) have been rotated upward 15° about the horizontal axis orthogonal to the page. *D*, Only the intrinsic vertical coordinate (for horizontal position) has been rotated. *E*, Only the intrinsic torsional coordinate has been rotated.

whereas the direction of drift remained orthogonal to the vertical coordinate in Listing's plane. In the final simulation (Fig. 4E) only the intrinsic torsional coordinate was rotated. Again, the direction of torsional drift remained approximately orthogonal to the intrinsic torsional coordinate (by also rotating upward), whereas the line of stability remained parallel to the intrinsic vertical coordinate. Thus, the model suggests that two separate and independent tests of the intrinsic integrator coordinate system can be applied to the torsional/vertical drift that occurs during pharmacological inactivation of the INC. First, the direction of drift should indicate the plane that contains the intrinsic coordinate axes for the damaged torsional and vertical integrators, and second, the line of stable positions should indicate the intrinsic vertical axis of the intact horizontal integrator.

Experimental coordinate test 1: direction of drift

This section examines the direction of drift, which (given the assumptions stated in the previous section) should be parallel to the horizontal plane containing the intrinsic coordinate axes of the torsional and vertical integrators. Figure 5A shows a horizontal (along the vertical axis) versus torsional plot of normal eye position vectors recorded during saccades and plotted in field coordinates. The range of positions relative to primary position clearly forms a planar distribution, which tilts back by 14.1° from the vertical field coordinate. This is Listing's plane plotted in field coordinates. Figure 5B shows data collected from the same animal on the same day, now 27 min after injection of muscimol into the left INC. Only postsaccadic drift is shown, using conventions similar to those in Figure 3 above. These sequences of drift form a series of parallel lines which start near Listing's plane (thick line) and proceed in a mainly clockwise direction. However, these lines also tilt upward from the torsional field coordinate. This tilt is consistently similar to the tilt of Listing's plane, so that the drift is orthogonal to Listing's

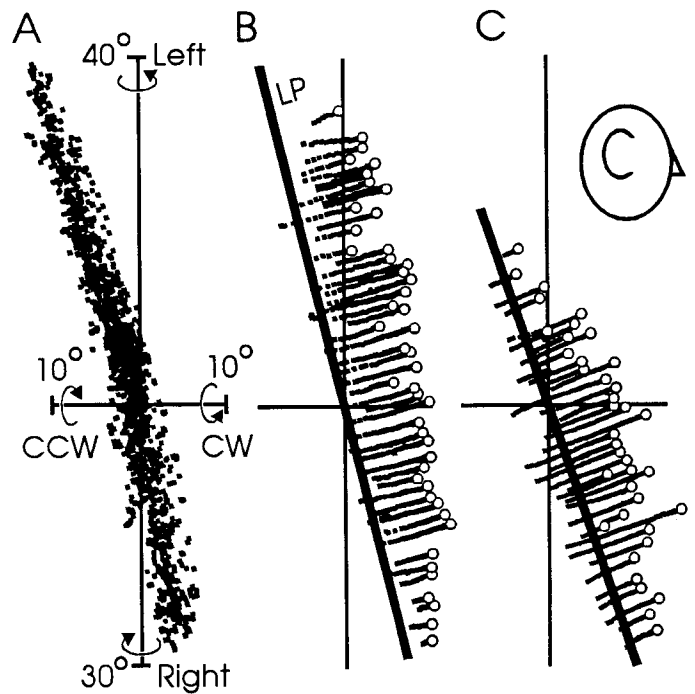


Figure 5. Direction of torsional drift after injection of muscimol into the INC. Horizontal positions and torsional positions (relative to primary position) are plotted in magnetic field coordinates. *A*, Normal eye positions during spontaneous saccades (i.e., Listing's plane). Torsional SDs were ~1° (Crawford and Vilis 1991). *B*, Same experiment, 27 min after injection of muscimol into the left INC. Positions during saccades have been deleted, and open circles are placed at the end-point of each drift sequence (which did not necessarily come to rest). The thick line indicates the plane of best fit to the data in *A*. *C*, An example from a different animal 33 min after injection of muscimol into the left INC. It is most accurate to state that these plots give the projection of drift onto the sagittal plane since vertical drift is also present, but is not visible in this view.

Table 1. Postsaccadic drift (\dot{E}) as a function of postsaccadic position (E)

	\dot{E}_T	\dot{E}_V	\dot{E}_H
E_T	-0.87 ± 0.18	0.20 ± 0.42	0.02 ± 0.12
E_V	0.04 ± 0.06	-0.61 ± 0.94	-0.03 ± 0.02
E_H	-0.08 ± 0.05	-0.08 ± 0.03	0.00 ± 0.02

Matrix values give the slopes (sec^{-1} , mean \pm SE across 25 experiments) of the time derivatives of torsional, vertical, and horizontal eye position ($\dot{E}_T, \dot{E}_V, \dot{E}_H$) as a function of torsional, vertical, and horizontal eye position (E_T, E_V, E_H) after injection of muscimol into the INC.

plane and parallel to the primary gaze direction. A similar example from a different animal (in which Listing's plane tilted up by 18.9°) is shown in Figure 5C. From these examples it is clear that the drift would appear to have horizontal components in the arbitrary field coordinate system that would disappear when transformed into Listing's coordinates, as illustrated in Figure 3.

To rigorously test the integrator coordinate system, the direction of the above drift was quantified. According to the model, it is change in eye position that indicates the intrinsic vertical coordinate. Therefore, the initial position of each sequence of drift (as illustrated in Fig. 5B,C) was subtracted from the final position to obtain overall "drift vectors." The initial position was taken as the first position where the angular speed during the preceding 10 msec was less than $60^\circ/\text{sec}$, whereas the final position was taken as the first position where the speed during the subsequent interval was greater than $60^\circ/\text{sec}$. Only drift vectors with torsional magnitudes greater than 2° were used for this analysis, yielding 25 experiments (10 in ART, 4 in CAS, 2 in LAR, and 9 in BAR) with an adequate number n of drift vectors for analysis (mean $n = 117.8$, SE = 16.7). The first postinjection 100 sec interval where this criteria was met was analyzed from each experiment, to minimize time of drug diffusion to other oculomotor structures. The average postinjection time interval for this data was 19.5 ± 14.2 min (± 1 SD). Since (1) the only difference between the effect of injecting muscimol into the right and left INC was the torsional offset where position settled (Crawford et al., 1991; Fukushima et al., 1992; Crawford and Vilis 1993), and (2) this was irrelevant for testing integrator coordinates (Fig. 4), data from right and left INC injections were combined.

Before applying the coordinate tests described in the previous section, the assumptions underlying these tests were evaluated by examining the eye position dependence of the drift. This was done by computing the slopes (by least squares regression across all drift sequences) between the three components of initial position (E) and the three components of initial rate of position change (\dot{E}) in each of the 25 experiments defined above. The means (\pm SE across all experiments) of these nine slopes are shown in Table 1. The largest entries were observed in the first two entries along the main diagonal ($E_T - \dot{E}_T, E_V - \dot{E}_V$) of Table 1, whereas the off-diagonal entries were small, indicating that there was little interdependence between nonsimilar components of eye position and eye drift. Neural integrator failure is characterized by centripetal drift in eye position at a rate that is approximately a linear function of current eye position (Robinson, 1989; Crawford and Vilis, 1993). This is normally quantified by the drift time constant (the time required to drift 63% of the way from initial position to the final resting position), which in a perfectly linear first order system would correspond

to the inverses of the entries along the main diagonal of Table 1 (i.e., the slope of E as a function of \dot{E}). Taking these inverses gives an average time constant of 1.16 seconds for torsional drift, and 1.63 sec for vertical drift, compared to a normal value of >20 sec (Robinson, 1989). As described in Crawford et al. (1991), these time constants often became even smaller as the postinjection interval progressed beyond 30 min. In contrast, the average time constant of horizontal drift could not be discriminated from the infinite, suggesting that the horizontal integrator was functioning normally. This lack of position dependence in the horizontal drift can be observed qualitatively in Figures 3 and 5; that is, the magnitude of the horizontal drift observed in the arbitrary coordinate systems was not dependent on horizontal eye position. Thus, the first prerequisite for our intrinsic coordinate tests, that damage be restricted to the torsional and vertical integrators, appeared to be satisfied by the data.

The second prerequisite for the coordinate test was that the integrator coordinates are fixed with respect to the head. An alternative possibility was that the intrinsic torsional coordinate is fixed with respect to the eye. If so, then the drift vectors should tilt up or down with the eye, that is, producing a horizontal drift dependent on vertical eye position. To evaluate this directly, regression fits between the angles of vertical eye position and the angles of upward tilt in the drift position-change vectors of each experiment were performed. The oculocentric scheme predicts a high correlation between these two angles and a slope of one, whereas the craniotopic scheme predicts zero correlation and a slope of zero. The experimentally measured correlation was only 0.08 ± 0.05 (mean \pm SE across all experiments) and the slope was only 0.10 ± 0.07 . Therefore, the subsequent analysis focused on the orientation of the intrinsic integrator coordinates within the craniotopic reference frame.

In order to determine the orientation of the intrinsic torsional and vertical coordinates of the integrator, the drift vectors of each experiment were averaged to produce a single mean drift vector. Figure 6A plots the upward tilt of these 25 mean drift vectors against the upward tilt of first order plane fits to the normal Listing's planes (both in field coordinates). The two were highly correlated ($r = 0.89$) with a slope near unity (1.10). In contrast there was little correlation ($r = 0.14$) between the drift vectors and the tilt of the stereotaxic planes with respect to field coordinates (Fig. 6B). In order to eliminate the arbitrary field coordinate system, the data are replotted in stereotaxic coordinates in Figure 6C. This plot shows that the orientation of Listing's plane (x-axis values) and the average drift direction (y-axis values) both varied over a range of $>30^\circ$ with respect to stereotaxic coordinates. However, they varied linearly together with a correlation coefficient of 0.85 and a slope of 0.94. Part of this correlation came from day-to-day covariations within the individual animals. For example, in the two animals with the largest data sample (BAR and ART), the tilt of Listing's plane about the interaural axis varied with respect to stereotaxic coordinates over ranges of 14.4° and 12.8° . The mean drift vectors showed similar day-to-day variations, yielding correlation coefficients of 0.81 and 0.80, respectively. In contrast, a plot of drift vectors versus stereotaxic planes in Listing's coordinates (Fig. 6D) gave little correlation ($r = 0.104$).

Experimental coordinate test 2: the range of stability

The second coordinate test developed above states that during torsional/vertical integrator failure, eye position will drift to-

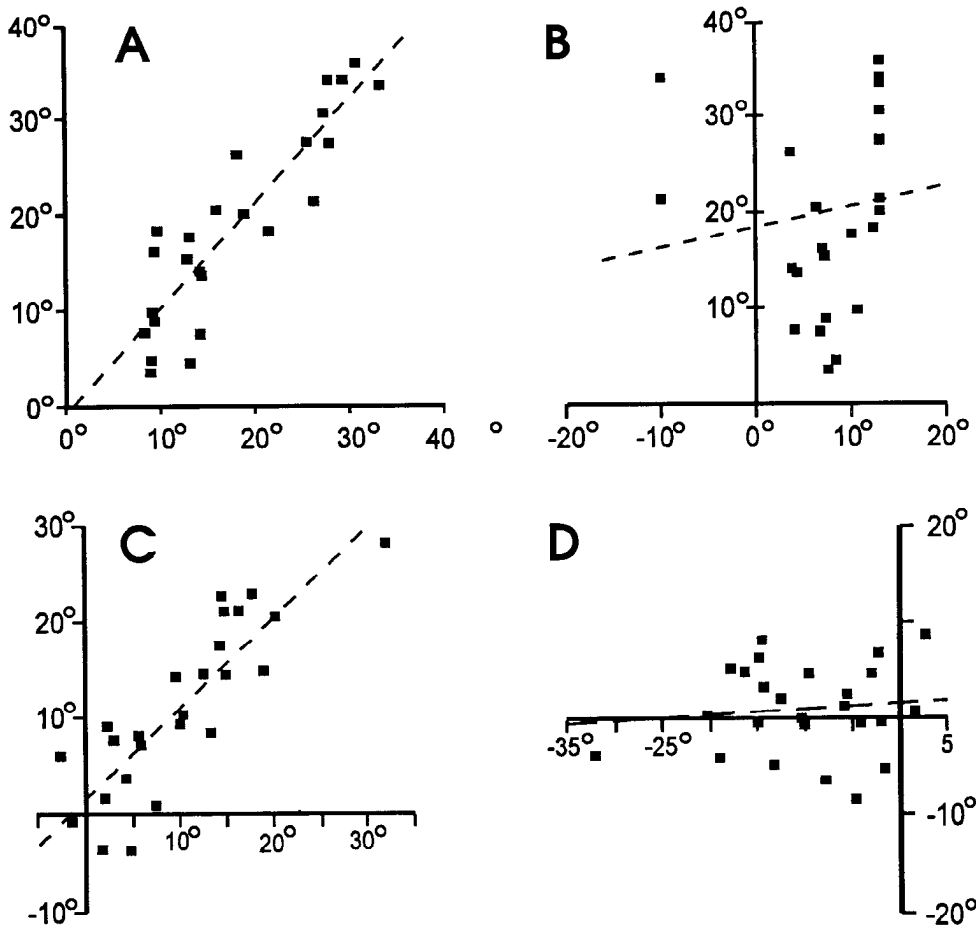


Figure 6. Mean directions of torsional drift in 25 experiments, as a function of Listing's plane and the stereotaxic planes. *Dashed lines* give the regression line fits to the data. *A*, Direction of drift (in magnetic field coordinates) as a function of the orientation of Listing's plane (in field coordinates). A positive angle denotes upward rotation about the horizontal coordinate axis. $r = 0.89$; slope = 1.10; y-intercept = -0.76° . *B*, Direction of drift (in field coordinates) as a function of the orientation of the stereotaxic planes (in field coordinates). $r = 0.14$; slope = 0.22; y-intercept = 18.50° . *C*, Direction of drift (in stereotaxic coordinates) as a function of the orientation of Listing's plane (in stereotaxic coordinates). $r = 0.85$; slope = 0.94; y-intercept = 1.57° . *D*, Direction of drift (in Listing's coordinates) as a function of the orientation of the stereotaxic planes (in Listing's coordinates). $r = 0.10$; slope = 0.06; y-intercept = 1.57° .

ward and settle at a range of positions parallel to the intrinsic vertical axis (for horizontal position) of the integrator. The range of torsional resting points was taken as those eye positions where torsional eye velocity was below $0.25^\circ/\text{sec}$ over the preceding 10 msec interval. Only data where the time constant of torsional drift was less than 1.5 sec, and where the torsional resting range had stabilized were included in this analysis. Twenty-six experiments fit this criteria: 10 in ART, 5 in CAS, 3 in LAR, and 8 in BAR. The first 100 sec interval that met the above criteria was analyzed from each experiment to minimize the effects of muscular spread to other brain structures. Across all of the 100 sec intervals analyzed, the average number of torsionally stable positions was 293 ± 23.85 (mean \pm SE).

Figure 7 gives an example of the range of positions that held during INC inactivation from two experiments. This figure plots eye position in Listing's coordinates, so that the vertical axis is contained in the plane fit to the normal saccadic eye positions measured at the beginning of the experiment, and this plane is viewed from the side (thick line). The vertical axis of the magnetic field coordinate system is indicated by the dashed line. As reported previously (Crawford et al., 1991; Fukushima et al., 1992; Crawford and Vilis, 1993), the range of stable torsional positions was usually shifted CCW during right INC inactivation (Fig. 7*A*) and CW during left INC inactivation (Fig. 7*B*). Of greater significance for the present investigation, these resting ranges were parallel to Listing's plane.

To quantify the orientation of these ranges, a plane of best fit was computed for each experiment. Figure 8*A* plots the orientation of these planes (backward tilt relative to the vertical field

coordinate) as a function of the backward tilt of Listing's plane. The correlation here ($r = 0.94$) is even higher than that of the drift direction, and again the slope is near unity (1.08). The correlation between the range of stability and the coronal stereotaxic plane (Fig. 8*B*) was more modest ($r = 0.46$, slope = 0.62). This modest relationship was apparently due to cross-correlation, because it disappeared when the data were transformed into Listing's coordinates (Fig. 8*D*; $r = 0.02$, slope = 0.01). In contrast the resting ranges and Listing's plane covaried ($r = 0.94$, slope = 0.97) over a range of $>30^\circ$ with respect to stereotaxic coordinates (Fig. 8*C*). Again, this correlation was also present in the day-to-day variations within individual animals. For example, the within-subject variations in ART and BAR yielded correlation coefficients of 0.88 and 0.68, respectively.

Orthogonality of integrator coordinates

Since the two sets of data aligned with Listing's plane and the primary gaze direction, they were expected to be mutually orthogonal. This was confirmed by quantitatively comparing the mean direction of torsional drift (presumably parallel to the intrinsic torsional coordinate) with the planes fit to the stable eye positions (presumably parallel to the intrinsic vertical axis). The angle obtained by subtracting the former from the latter, across all individual experiments in which both were quantified ($n = 23$), was $91.85^\circ \pm 1.21^\circ$ (mean \pm SE). This value becomes even closer to orthogonality if averages were taken across the four mean values for each animal ($90.91^\circ \pm 1.52^\circ$).

Figure 9 qualitatively summarizes the above data (Figs. 5–8)

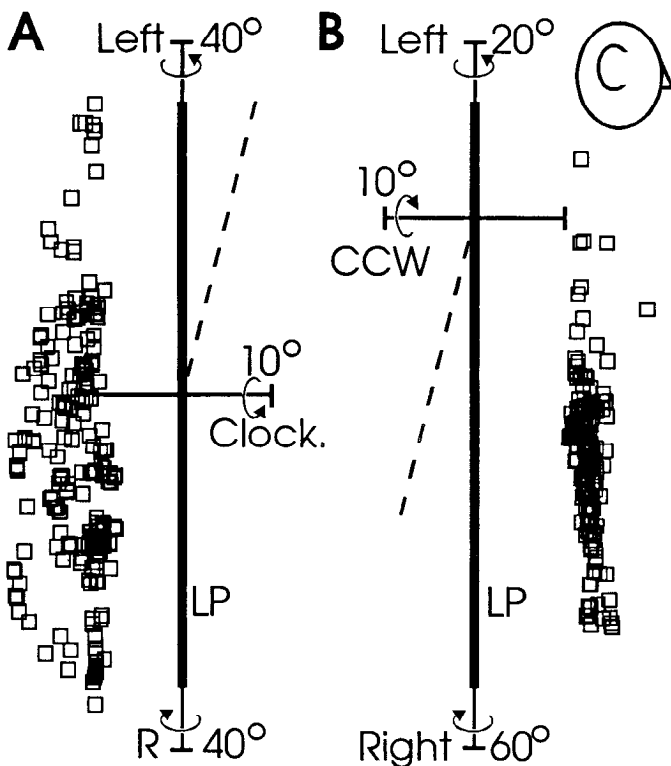


Figure 7. Range of stable eye positions after unilateral injection of muscimol into the INC. Torsional and horizontal (along the vertical axis) components of eye position vectors are plotted in Listing's coordinates (i.e., the vertical axis is embedded in Listing's plane). Eye positions (\square) are only plotted when eye velocity had dropped below $0.25^\circ/\text{sec}$ (see text in Results). *A*, Thirty-one min after injection into the right INC. *B*, Ten min after injection into the left INC.

for all experiments and animals. The mainly vertical wedges give the axes of best fit to the ranges of stable torsion (mean \pm 1 SE across all experiments in each animal). The mainly horizontal wedges show the average directions of torsional drift (mean \pm 1 SE across all experiments in each animal). In stereotaxic coordinates (Fig. 9*A*), the data were variable and poorly aligned, although the intrinsic orthogonality between the two sets of data in each animal is evident in the figure. When the same data were transformed into Listing's coordinates (Fig. 9*B*), the variability within and between animals was greatly reduced, revealing a remarkable alignment with Listing's plane and the primary gaze direction. Averaged across the four mean values of each animal (illustrated in Fig. 9), the plane that contained the direction of drift was rotated upward by only $0.06^\circ \pm 1.52^\circ$ (mean \pm SE) from the normal to Listing's plane. Similarly, the line of stable positions was aligned within $0.98^\circ \pm 1.81^\circ$ (mean \pm SE) from Listing's plane.

Discussion

The results of this investigation suggest that the oculomotor neural integrator does use a definable coordinate system, but the precise orientation of this coordinate system is only evident at the level of integrator cell populations. This result relies on the prerequisite observation, confirmed in this study, that the integrator for horizontal eye position is functionally (and anatomically) independent from the integrators for torsional and vertical position. As a result of this segregation, integrator failure will produce eye position drift that is (1) parallel to the intrinsic

coordinate axes of the damaged part(s) of the integrator, and (2) settles toward a range that is parallel to the intact coordinate axis (Fig. 4). These phenomena were demonstrated with the use of a quaternion model of the saccade generator, but they are inherent properties of integrating in three dimensions and are therefore representation independent. The experimental test results suggest that the oculomotor integrator uses an orthogonal coordinate system that is fixed within the craniotopic reference frame and aligned with Listing's plane.

These results are consistent with the view that the INC controls coordinate axes (for vertical and torsional eye position) that lay in a horizontal plane. During INC inactivation, eye position vectors drifted parallel to this horizontal plane. The data presented here did not elucidate the orientation of the coordinate axes within this plane. However, previous investigations suggest that the INC does not use separate coordinates for vertical and torsional position, but instead combines torsional and vertical control like the eye muscle and semicircular canal coordinate systems (i.e., viewed from above the head, the coordinate axes would resemble a \times rather than a $+$) (Fukushima et al., 1990a, 1992; Crawford et al., 1991). The observed independence of horizontal drift with respect to vertical eye position suggests that these coordinate axes are fixed with respect to the head. Finally, the direction of drift was orthogonal to the measured ranges of stable eye positions; a nontrivial observation (see Fig. 4*D,E*). This suggests that the horizontal coordinate axes for torsional and vertical eye position are orthogonal, in the familiar Euclidian sense, to the vertical coordinate axis for horizontal position (presumably controlled by the nucleus prepositus hypoglossi region) (Cannon and Robinson, 1987; Cheron and Godaux, 1987).

Despite its resemblance to the muscle and canal coordinate system, the integrator coordinate system does not appear to align best with any anatomic system. Both the directions of drift after INC inactivation and the orientations of the resting position range varied about the interaural axis with respect to stereotaxic coordinates by as much as 30° between animals (Figs. 6*C*, 8*C*). It is unlikely that the axes of rotation controlled by the eye muscles and semicircular canals could have varied to this extent. For example, the anatomically measured planes of the medial and lateral rectus muscles varied about the interaural axis over a range of 6.7° and 7.8° , respectively, in four monkeys (J. I. Simpson, personal communication). Furthermore, it is unlikely that these muscle planes could vary from day to day in one animal to the extent observed in the drift vectors and ranges of stability during INC inactivation. However, Listing's plane is known to vary widely in orientation both between subjects and over time in individual subjects (von Helmholtz, 1867; Ferman et al., 1987; Tweed and Vilis, 1990a). The present study demonstrates a correlation between the variations (both within and between subjects) of integrator coordinates and Listing's plane. In particular, the intrinsic coordinate axes for torsional and vertical rotation (controlled by the INC) lie in the horizontal plane orthogonal to Listing's plane, and the remaining vertical coordinate for horizontal rotation (presumably controlled by the nucleus prepositus hypoglossi) aligns with Listing's plane.

A similar alignment between intrinsic neural coordinates and Listing's plane was recently observed in populations of short lead oculomotor burst neurons of the mesencephalic rostral interstitial nucleus of the medial longitudinal fasciculus (riMLF) (Crawford and Vilis, 1992), which project directly to the INC (Moschovakis et al., 1991). Since burst neurons provide the

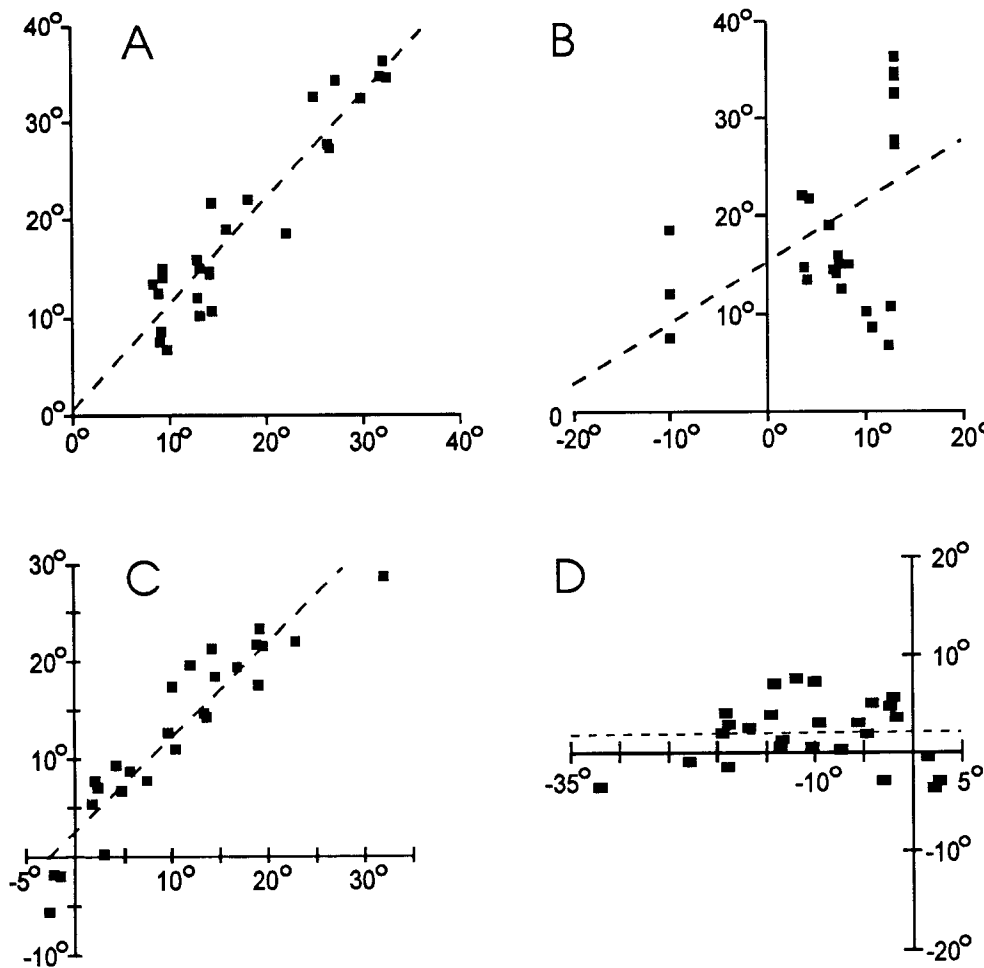


Figure 8. Orientations of stability ranges (see Results) in 26 experiments, as a function of Listing's plane and the stereotaxic planes. *Dashed lines* give the regression line fits to the data. *A*, Orientation of stability range (in magnetic field coordinates) as a function of the orientation of Listing's plane (in field coordinates). A positive angle denotes upward rotation about the horizontal coordinate axis. $r = 0.94$; slope = 1.08; y-intercept = 0.94°. *B*, Orientation of stability range (in field coordinates) as a function of the orientation of the stereotaxic planes (in field coordinates). $r = 0.46$; slope = 0.62; y-intercept = 15.28°. *C*, Orientation of stability range (in stereotaxic coordinates) as a function of the orientation of Listing's plane (in stereotaxic coordinates). $r = 0.94$; slope = 0.97; y-intercept = 2.55°. *D*, Orientation of stability range (in Listing's coordinates) as a function of the orientation of the stereotaxic planes (in Listing's coordinates). $r = 0.02$; slope = 0.01; y-intercept = 2.11°.

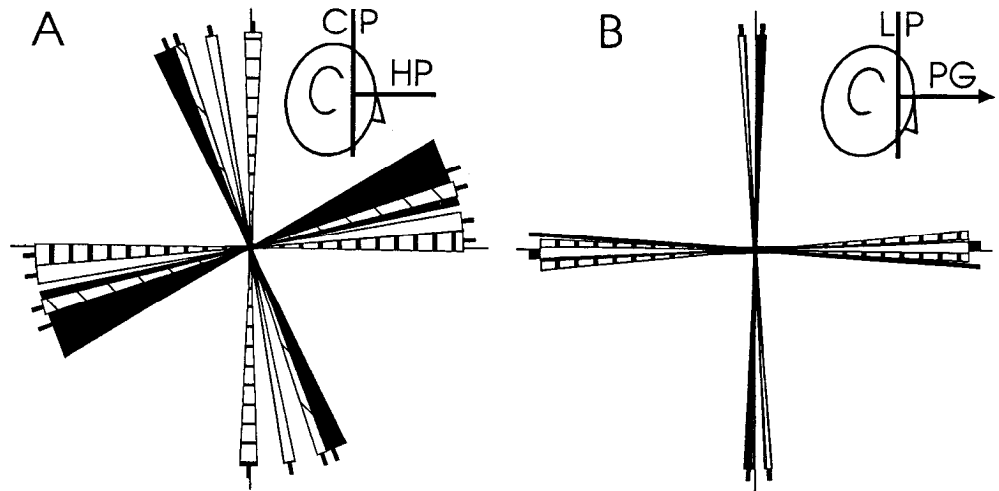
movement command for saccades in Listing's plane (Tweed and Vilis, 1990b), their activity is similarly constrained by Listing's law. Burst neurons also utilize a muscle- or canal-like coordinate system, in that they are arranged into two separate populations that control CW-up and CW-down eye rotations in the right riMLF, and two populations that control CCW-up and CCW-down rotations in the left riMLF (Hepp et al., 1988; Crawford and Vilis, 1992). However, the coordinates axes controlled by these burst neuron populations did not appear to align with either muscle or canal coordinates (Crawford and Vilis, 1992). Instead, unilateral stimulation of these populations produced mainly torsional rotations of the eyes about axes in the horizontal plane orthogonal to Listing's plane. Furthermore, muscimol inactivation of the riMLF leaves an intact vertical axis of rotation, presumably generated in the pons (Luschei and Fuchs, 1971), that is aligned with Listing's plane (Crawford and Vilis, 1992). Therefore, at least two premotor structures whose activity is constrained by Listing's law, the oculomotor integrator and short lead burst neurons, use a population coordinate system that resembles that of the muscles and canals but is aligned with Listing's plane.

Thus, contrary to a recent suggestion (Robinson, 1992), brain coordinate systems are not just a trivial by-product of anatomic geometries. Most previous investigations of sensorimotor transformations have assumed a rather direct transformation between sensory and muscular coordinate systems, which is probably the case for geometrically simple transformations like the

vestibulo-ocular reflex (Robinson, 1985; Simpson and Graf, 1985). The present study corroborates the more recent view that "abstract" intermediate coordinate systems are used to represent the neural commands for more complex behaviors (Flanders and Soechting, 1990; Masino and Knudsen, 1993). Furthermore, this investigation suggests that these abstract coordinate systems are chosen to optimally suit these behavioral commands. The generation of specific behaviors always requires a selection amongst the infinitely possible set of motor commands (Crawford and Vilis, 1994). The present investigation examines just one simple example of such a selection: Listing's law constrains the neural integrator to encode only a two-dimensional subset of the possible three-dimensional space of eye positions. Thus, the brain could simplify its task considerably by parameterizing movement commands along coordinates that align with such parameters that emerge in behavior.

Alignment between Listing's plane and both burst neuron and integrator coordinates has in fact been implicitly incorporated into all previous schemes and models of neural mechanism for Listing's law (Robinson and Zee, 1981; Hepp, 1990; Tweed and Vilis, 1990b; Clement, 1991; Schnabolk and Raphan, 1993). This arises naturally because it gives a specific symmetry that illustrates the means by which behavioral coordinate systems simplify neural computations: in order for the integrator to encode positions in Listing's plane it always encodes zero torsion in its intrinsic coordinate system. Otherwise, the integrator would have to encode finite values of torsion in its intrinsic coordinates

Figure 9. Qualitative summary of coordinate tests. The mainly *vertical lines* give the mean (across experiments) orientation of the range of stability for each of the four animals. The mainly *horizontal lines* give the mean direction of torsional drift (more accurately the plane of torsional-vertical drift viewed edge-on from the side) for each animal. Superimposed on these lines are color-coded wedges that give ± 1 SEM for each animal. *A*, Data plotted in stereotaxic coordinates, that is, viewed orthogonal to the coronal plane (*CP*) and horizontal plane (*HP*). *B*, Data plotted in Listing's coordinates, that is, viewed orthogonal to Listing's plane (*LP*) and the primary gaze direction (*PG*).



in order to encode zero torsion in Listing's plane. For example, suppose that the horizontal integrator encoded pure horizontal rotation about a vertical axis that was rotated upward (i.e., tilted backward) from Listing's plane. Compared to this coordinate system, the vector for a leftward eye position in Listing's plane would tilt forward, that is, have a clockwise component, as in Figure 1*B*. This would require coactivation of the clockwise/up and clockwise/down tuned neurons of the right INC to hold eye position in Listing's plane, and similarly left INC cells would have to be activated for rightward eye positions. No such systematic horizontal eye position dependence has been observed in single-unit activity of the INC (King et al., 1981; Fukushima et al., 1990b). Thus, perhaps surprisingly, alignment of integrator coordinates is required for the "horizontal" integrator to uniquely encode horizontal eye position in Listing's plane, and for the "vertical" integrator to encode vertical eye position uniquely (through bilaterally equal activation of "up" or "down" populations with opposite torsional effects).

The question remains how integrator coordinates would come to align thus with Listing's plane. The fundamental anatomic separation between the horizontal and vertical integrator is probably predetermined genetically, but several specific hypotheses have been offered to explain their muscle/canal-like organization: (1) it may be imposed by inputs from the semicircular canals (Robinson and Zee 1981), perhaps through a developmental rule that competitively strengthens synaptic inputs (to an integrator neuron) with similar directional activity at the expense of dissimilar inputs, (2) visual calibration of the integrator (Robinson 1987, 1985, 1992) would favor a one-to-one synaptic mapping between canals and muscles in the same anatomic plane, and (3) this coordinate system has been demonstrated to satisfy both orthogonality and bilateral anatomic symmetry, two factors of possible developmental importance (Robinson, 1985; Simpson and Graf, 1985; Crawford et al., 1991; Crawford and Vilis, 1992). However, orthogonality and anatomic symmetry would still be satisfied if this coordinate system were rotated through any angle about the interaural axis. The question is, what rotates it into alignment with Listing's plane?

A likely candidate for this aligning role is the bilateral symmetry of neural activity that alignment with Listing's plane uniquely provides. The commissural connections between the two sides of the INC could monitor the asymmetries in activity

that would result from misalignment of integrator coordinates with Listing's plane. The resulting error signal could be used to adjust the synaptic strengths of integrator outputs until alignment is achieved. In general, this alignment would require the INC to project to the horizontal eye muscles as well as the torsional/vertical muscles, and similarly the horizontal integrator would require some projections to the torsional/vertical muscles. Presumably, alignment would originate when the integrator's saccade-related inputs first establish patterns of activity consistent with Listing's law. However, the results of the present study suggest that the plasticity necessary for realignment persists into adulthood. To the extent that Listing's plane might be altered in response to training or injury, so should the integrator coordinate system.

In summary, this investigation suggests or is consistent with several general conclusions. First, it demonstrates the utility of modeling brain function and dysfunction using explicit mathematical operations (such as integration) in explicit coordinate systems. However, simple computational models may only be representative of the overall function of task-related neuron populations. The reason that neuron populations are more easily described by simple rule-based models could be that developmental rules may only apply to the overall behavior of neuron populations, being blind to stochastic variations within these populations (as demonstrated in connectionist neural network models). Since some of these developmental rules appear to depend on neural signaling activity itself, it should not be surprising if neuron population coordinates are influenced by constraints imposed on their activity by generating specific behaviors. In the oculomotor system this appears to give rise to a simplifying encoding of behavioral commands along coordinates that align with basic elements inherent in the behavior. Finally, this investigation demonstrates that measurement of movement deficits in arbitrary coordinate systems will give misleading results (such as the superfluous horizontal drift observed during INC inactivation). Fortunately, the correct coordinate systems might sometimes be inferred from noninvasive behavioral measurements.

References

- Büttner U, Büttner-Ennever JA, Henn V (1977) Vertical eye unit related activity in the rostral mesencephalic reticular formation of the alert monkey. *Brain Res* 130:239–252.

- Cannon SC, Robinson DA (1987) Loss of the neural integrator of the oculomotor system from brainstem lesions in the monkey. *J Neurophysiol* 57:1383-1409.
- Cheron G, Godaux E (1987) Disabling of the oculomotor integrator by kainic acid injections in the prepositus-vestibular complex of the cat. *J Physiol (Lond)* 394:267-290.
- Crawford JD, Vilis T (1991) Axes of eye rotation and Listing's law during rotations of the head. *J Neurophysiol* 65:407-423.
- Crawford JD, Vilis T (1992) Symmetry of oculomotor burst neuron coordinates about Listing's plane. *J Neurophysiol* 68:432-448.
- Crawford JD, Vilis T (1993) Modularity and parallel processing in the oculomotor integrator. *Exp Brain Res* 96:443-456.
- Crawford JD, Cadera W, Vilis T (1991) Generation of torsional and vertical eye position signals by the interstitial nucleus of Cajal. *Science* 252:1551-1553.
- Ezure K, Graf W (1984) A quantitative analysis of the spatial organization of the vestibulo-ocular reflexes in lateral- and frontal-eyed animals. I. Orientation of the semicircular canals and extraocular muscles. *Neuroscience* 12:85-93.
- Ferman L, Collewijn H, Van den Berg AV (1987a) A direct test of Listing's law. I. Human ocular torsion measured in static tertiary positions. *Vision Res* 27:929-938.
- Flanders M, Soechting JF (1990) Parcellation of sensorimotor transformations for arm movements. *J Neurosci* 10:2420-2427.
- Fukushima K (1987) The interstitial nucleus of Cajal and its role in control of movements of head and eyes. *Prog Neurobiol* 29:107-192.
- Fukushima K, Harada C, Fukushima J, Suzuki Y (1990a) Spatial properties of vertical eye movement-related neurons in the region of the interstitial nucleus of Cajal. *Exp Brain Res* 79:25-42.
- Fukushima K, Fukushima J, Harada C, Ohashi T, Kase M (1990b) Neuronal activity related to vertical eye movement in the region of the interstitial nucleus of Cajal in alert cats. *Exp Brain Res* 79:43-64.
- Fukushima K, Ohashi T, Fukushima J, Kase M (1992) Ocular torsion produced by unilateral chemical inactivation of the interstitial nucleus of Cajal in chronically labyrinthectomized cats. *Neurosci Res* 13:301-305.
- Haslwanter T, Hepp K, Straumann D, Dursteller MR, Hess BJM (1992) Smooth pursuit eye movements obey Listing's law in the monkey. *Exp Brain Res* 87:470-472.
- Hepp K (1990) On Listing's law. *Commun Math Phys* 132:285-292.
- Jürgens R, Becker W, Kornhuber HH (1981) Natural and drug induced variations of velocity and duration of human saccadic eye movements: evidence for a control of the neural pulse generator by local feedback. *Biol Cybern* 39:87-96.
- King WM, Fuchs AF, Magnin M (1981) Vertical eye movement-related responses of neurons in midbrain near interstitial nucleus of Cajal. *J Neurophysiol* 46:549-562.
- Leigh RJ, Zee DS (1991) Contemporary neurology series, The neurology of eye movements, 2d ed. Philadelphia: Davis.
- Luschei ES, Fuchs AF (1972) Activity of brain stem neurons during eye movements of alert monkeys. *J Neurophysiol* 35:445-461.
- Masino T, Knudsen EI (1993) Orienting head movements resulting from electrical microstimulation of the brainstem tegmentum in the barn owl. *J Neurosci* 13:351-370.
- Minken AWH, Van Opstal AJ, Van Gisbergen JAM (1993) Three-dimensional analysis of strongly curved saccades elicited by double-step stimuli. *Exp Brain Res* 93:521-533.
- Moschovakis AK, Scudder CA, Highstein SM, Warren JD (1991) Structure of the primate oculomotor burst generator. II. Medium lead burst neurons with downward on-directions. *J Neurophysiol* 65:218-229.
- Robinson DA (1968) Eye movement control in primates. *Science* 161:1219-1224.
- Robinson DA (1975) Oculomotor control signals. In: Basic mechanisms of ocular motility and their clinical implications (Bach-y-Rita P, Lennerstrand G, eds), pp 337-374. Oxford: Pergamon.
- Robinson DA (1985) The coordinates of neurons in the vestibulo-ocular reflex. In: Adaptive mechanisms in gaze control. Facts and theories (Berthoz A, Melvill Jones G, eds), pp 297-311. Amsterdam: Elsevier.
- Robinson DA (1989) Integrating with neurons. *Annu Rev Neurosci* 12:33-45.
- Robinson DA (1992) Implications of neural networks for how we think about brain function. *Behav Brain Sci* 15:644-655.
- Robinson DA, Zee DS (1981) Theoretical considerations of the function and circuitry of various rapid eye movements. In: Progress in oculomotor research (Fuchs A, Becker W, eds), pp 3-9. New York: Elsevier/North-Holland.
- Schnabolk C, Raphan T (1993) Model of three dimensional velocity-position transformation in oculomotor control. *Soc Neurosci Abstr* 19:1592.
- Shantha TR, Manocha SL, Bourne GH (1968) A stereotaxic atlas of the Java monkey brain. New York: Karger.
- Shatz CJ (1992) The developing brain. *Sci Am* 267:60-67.
- Simpson JI, Graf W (1985) The selection of reference frames by nature and its investigators. In: Adaptive mechanisms in gaze control. Facts and theories (Berthoz A, Melvill Jones G, eds), pp 3-16. Amsterdam: Elsevier.
- Soechting JF, Flanders M (1992) Moving in three-dimensional space: frames of reference, vectors, and coordinate systems. *Annu Rev Neurosci* 15:167-192.
- Straube A, Kurzan R, Büttner U (1991) Differential effects of bicuculline and muscimol microinjections into the vestibular nuclei on simian eye movements. *Exp Brain Res* 86:347-358.
- Tweed D, Vilis T (1987) Implications of rotational kinematics for the oculomotor system in three dimensions. *J Neurophysiol* 58:832-849.
- Tweed D, Vilis T (1990a) Geometric relations of eye position and velocity vectors during saccades. *Vision Res* 30:111-127.
- Tweed D, Vilis T (1990b) The superior colliculus and spatiotemporal translation in the saccadic system. *Neural Networks* 3:75-86.
- Tweed D, Cadera W, Vilis T (1990) Computing three dimensional eye position quaternions and eye velocity from search coil signals. *Vision Res* 30:97-110.
- Tweed D, Fetter M, Andreadaki S, Koenig E, Dichgans J (1992) Three-dimensional properties of human pursuit eye movements. *Vision Res* 32:1225-1238.
- von Helmholtz H (1867) *Handbuch der Physiologischen optik*, Vol 3, 1st ed. Hamburg: Voss. Reprinted in: *Treatise on physiological optics* (Southall JPC, trans). *Opt Soc Am* 3:44-51, 1925.
- Van Opstal AJ, Hepp K, Hess BJM, Straumann D, Henn V (1991) Two- rather than three-dimensional representation of saccades in monkey superior colliculus. *Science* 252:1313-1315.
- Westheimer G (1957) Kinematics of the eye. *J Opt Soc Am* 47:967-974.
- Yokota J, Reisine H, Cohen B (1992) Loss of integrator function after injection of GABAergic substances into the prepositus hypoglossi nuclei (PPH). *Soc Neurosci Abstr* 18:509.